

## Reversible Single-Crystal-to-Single-Crystal Transformation from Mononuclear Complex to Fourfold Interpenetrated MOF with Selective Adsorption on CO<sub>2</sub>

Min-Min Liu, Yan-Lin Bi, Qin-Qin Dang, Xian-Ming Zhang\*

School of Chemistry & Material Science, Shanxi Normal University, Linfen 041004, P. R. China.

**Table S1.** Crystal Data and Structure Refinement for Complexes **1** and **2**.

Identification code	<b>1</b>	<b>2</b>
Empirical formula	C <sub>18</sub> H <sub>20</sub> CuN <sub>6</sub> O <sub>8</sub>	C <sub>18</sub> H <sub>12</sub> CuN <sub>6</sub> O <sub>4</sub>
Formula weight	511.94	439.88
Temperature/K	293(2)	293(2)
Crystal system	triclinic	orthorhombic
Space group	P-1	Pnna
a/Å	6.2530(15)	13.0574(5)
b/Å	7.052(2)	9.9328(4)
c/Å	12.075(3)	17.5051(6)
α/°	79.90(2)	90.00
β/°	88.21(2)	90.00
γ/°	71.13(2)	90.00
Volume/Å <sup>3</sup>	495.9(2)	2270.36(15)
Z	1	4
ρ <sub>calc</sub> /mg/mm <sup>3</sup>	1.714	1.287
m/mm <sup>-1</sup>	1.165	0.994
F(000)	263.0	892.0
Crystal size/mm <sup>3</sup>	0.14 × 0.13 × 0.12	0.24 × 0.22 × 0.20
2θ	6.2 to 52°	5.66 to 51.98°
Reflections	3061	5397
Ind.refls.	1923	2244
Data/restraints/parameters	1923/0/153	2244/0/132
Goodness-of-fit on F <sup>2</sup>	1.061	1.062
R <sub>1</sub>	0.0787/0.1649	0.0423/0.0667
wR <sub>2</sub>	0.1076/0.1842	0.1198/0.1292
peak/hole / e Å <sup>-3</sup>	0.82/-0.72	0.25/-0.24

<sup>a</sup>  $R_1 = \sum ||F_o| - |F_c|| / \sum |F_o|$ ,  $wR_2 = [\sum w(F_o^2 - F_c^2)^2 / \sum w(F_o^2)^2]^{1/2}$

**Table S2.** Bond Lengths and angles for **1** and **2**.

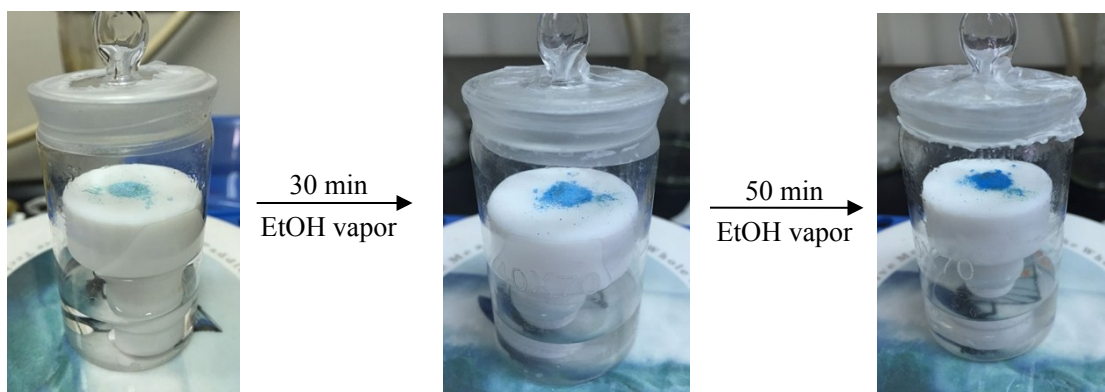
Complex 1			
Cu(1)-O(1W)	2.035(4)	Cu(1)-O(3Wa)	2.378(4)
Cu(1)-O(1Wa)	2.035(4)	Cu(1)- N(2)	2.005(4)
Cu(1)-O(3W)	2.378(4)	Cu(1)-N(2a)	2.005(4)
O(1Wa)-Cu(1)- O(1W)	180.00(3)	N(2a)-Cu(1)- O(1)	86.53(16)
O(3Wa)-Cu(1)- O(1Wa)	92.16(16)	N(2)-Cu(1)- O(1Wa)	86.53(16)
O(1W)-Cu(1)- O(3Wa)	87.84(16)	N(2a)-Cu(1)- O(3W)	88.04(16)
O(1W)-Cu(1)- O(3W)	92.16(16)	N(2)-Cu(1)- O(3W)	88.04(16)
O(1Wa)-Cu(1)- O(3W)	87.84(16)	N(2a)-Cu(1)- O(3W)	91.96(16)
O(3Wa)-Cu(1)- O(3W)	180.0(17)	N(2)-Cu(1)- O(3Wa)	91.96(16)
N(2a)-Cu(1)- O(1Wa)	93.47(16)	N(2a)-Cu(1)- N(2)	180.0(2)
N(2)-Cu(1)- O(1W)	93.47(16)		

Symmetry codes: a)  $-x+1, -y+1, -z$

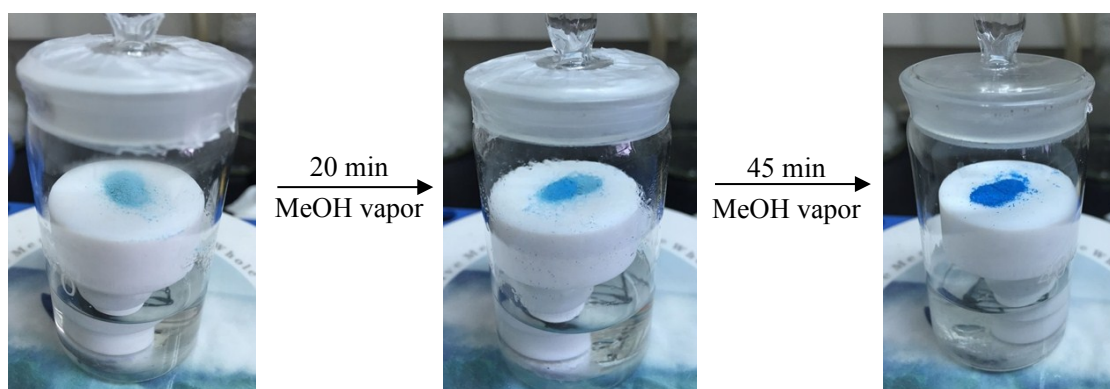
Complex 2			
Cu(1)-O(1a)	1.979(2)	Cu(1)-N(3b)	1.991(3)
Cu(1)-O(1)	1.979(2)	Cu(1)-N(3c)	1.991(3)
O(1)-Cu(1)-O(1a)	90.26(13)	O(1a)-Cu(1)- N(3c)	89.79(10)
O(1)-Cu(1)-N(3b)	89.79(10)	O(1)-Cu(1)- N(3c)	165.71(9)
O(1a)-Cu(1)-N(3b)	165.71(9)	N(3c)-Cu(1)- N(3b)	93.65(16)

Symmetry codes: a)  $-x+3/2, -y, +z$  b)  $-x+1, y-1/2, z+1/2$  c)  $x+1/2, -y+1/2, z+1/2$

Heating the ethanol/methanol solution in the weighing bottle (40×70mm) can generate stable steam with the water-bath method at 85°C and 80°C. Then the samples of **1** is put on the preheated platform above the solution. Finally, the bottle should be sealed to watch the changes of mononuclear **1**.



(a)



(b)

**Figure S1.** The SCSC transformation from light blue crystals of **1** to blue crystals of **2** in EtOH vapor at 85°C (a) and in MeOH vapor at 80°C (b).

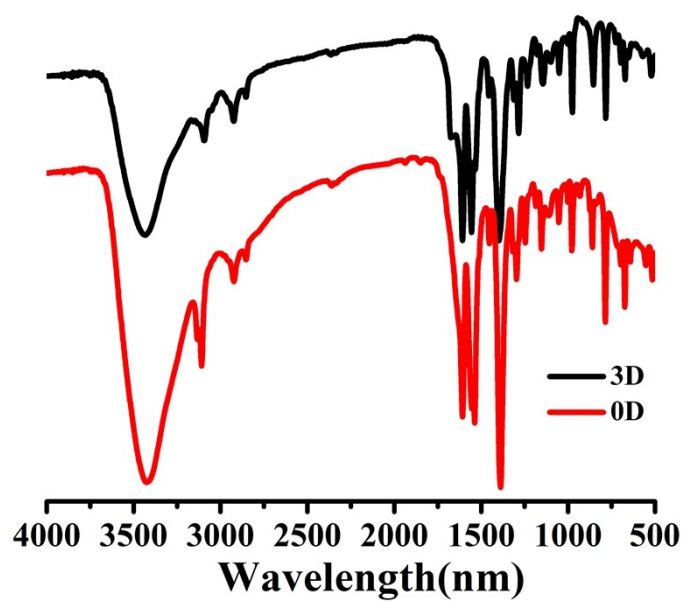


**Figure S2.** IR spectra of **1** (red) and **2** (black) in KBr pellet.

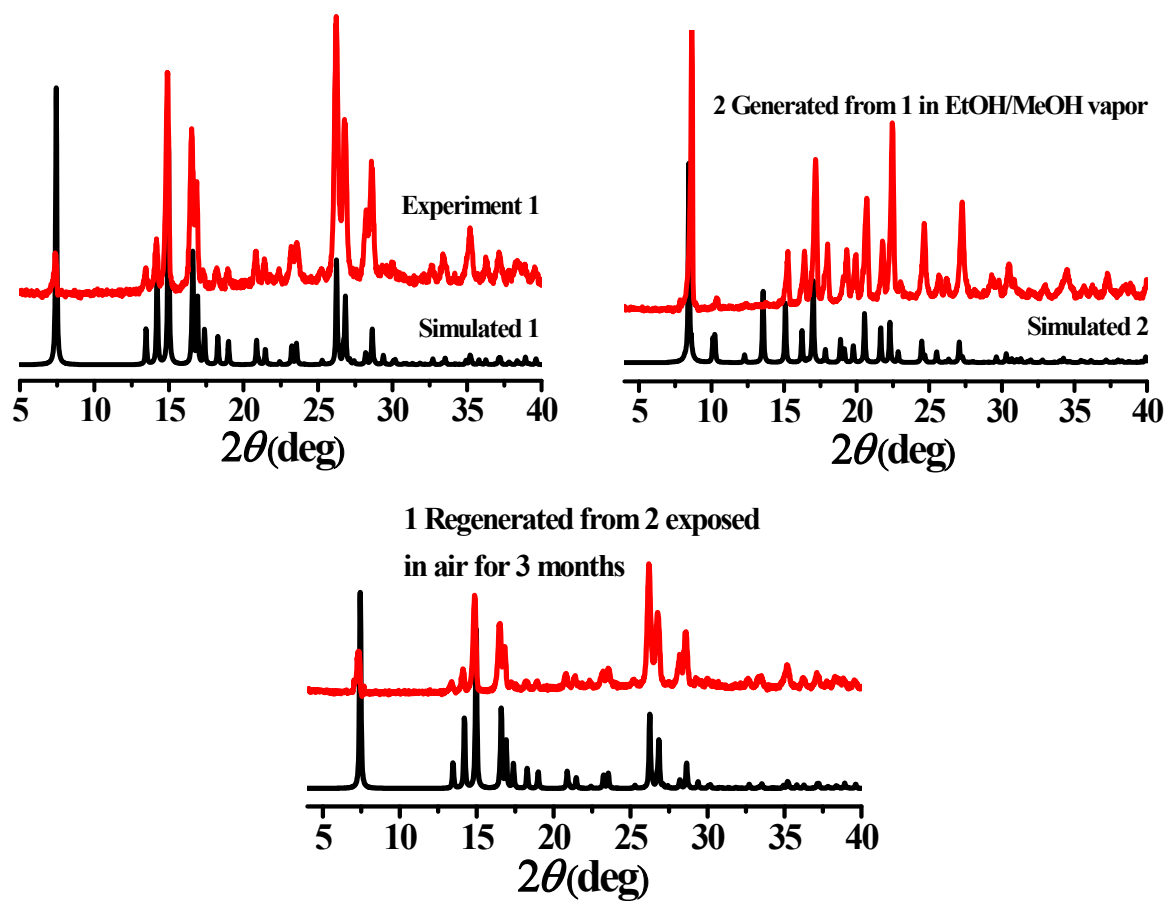
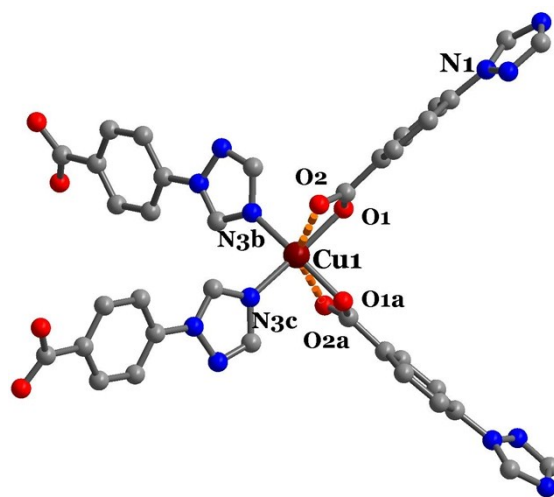
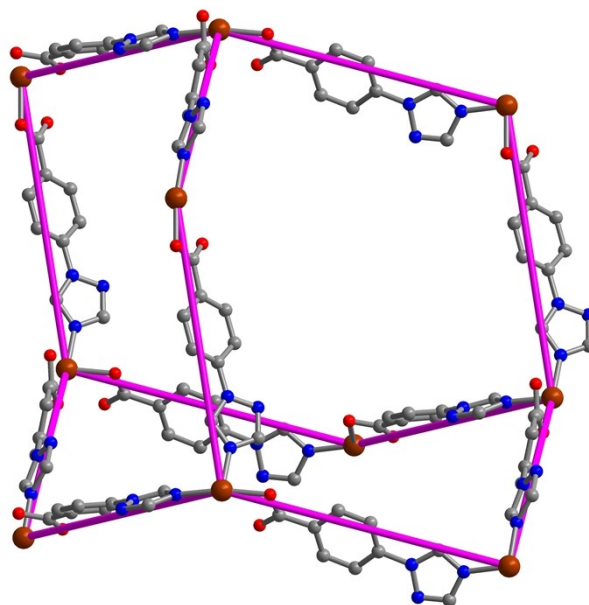


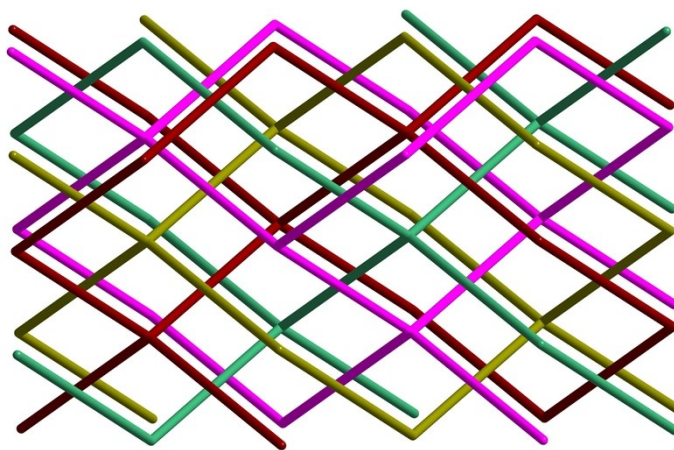
**Figure S3.** PXRD patterns showing reversible SCSC transformation between 1 and 2.



(a)



(b)



(c)

**Figure S4.** View of coordination environment of Cu atom (a), single diamondoid cage (b) and Fourfold interpenetrated diamond net (c) of **2**.

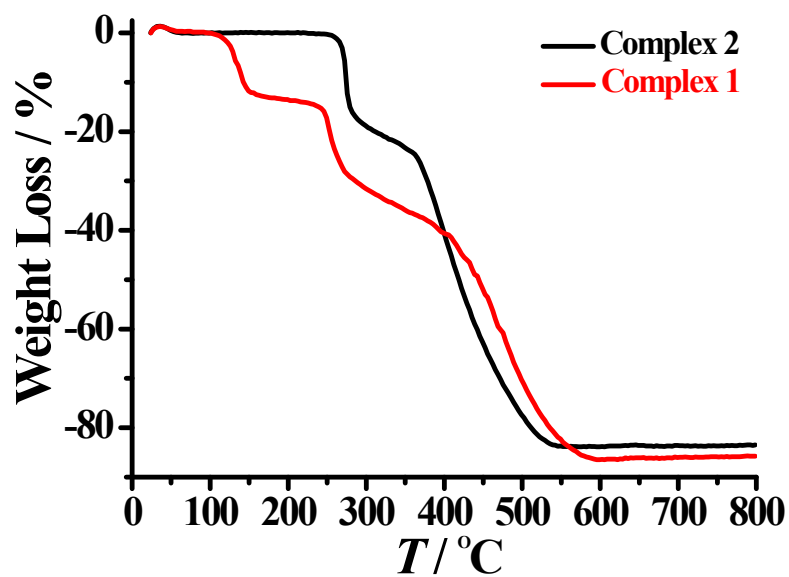


**Figure S5.** The TGA plots of complex 1 (red) and 2 (black) at the heating rate of 5°C per min in air.

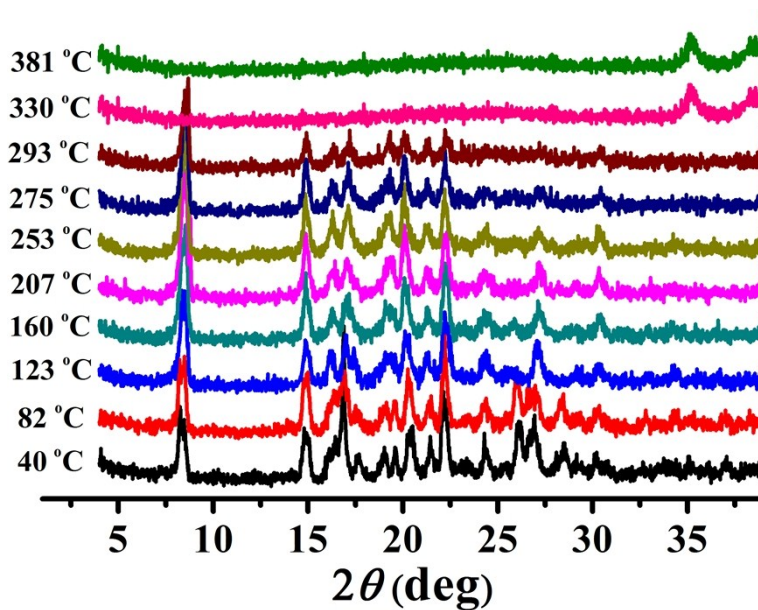
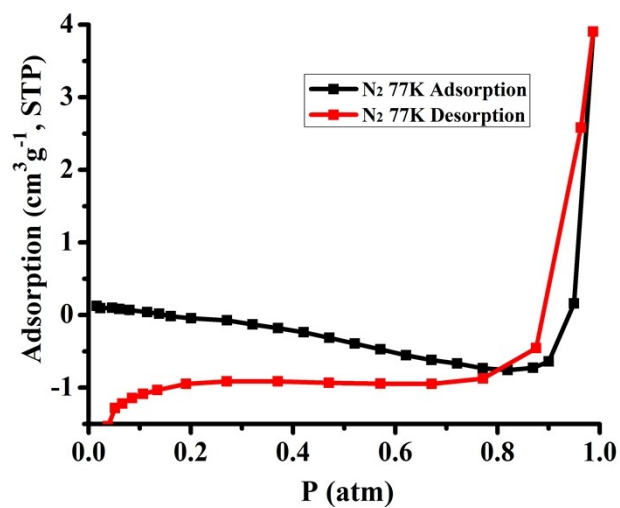
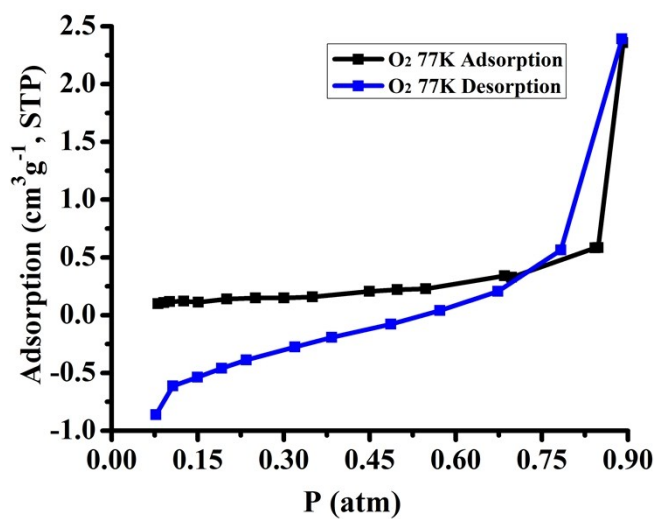


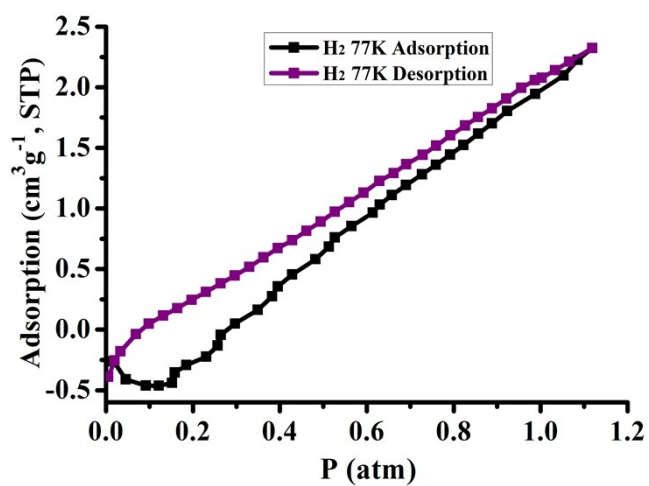
**Figure S6.** The temperature varied PXRD patterns for 2.



(a)



(b)



(c)

**Figure S7.**  $N_2$  (a),  $O_2$  (b) and  $H_2$  (c) adsorption and desorption isotherms of **2** in 77K.

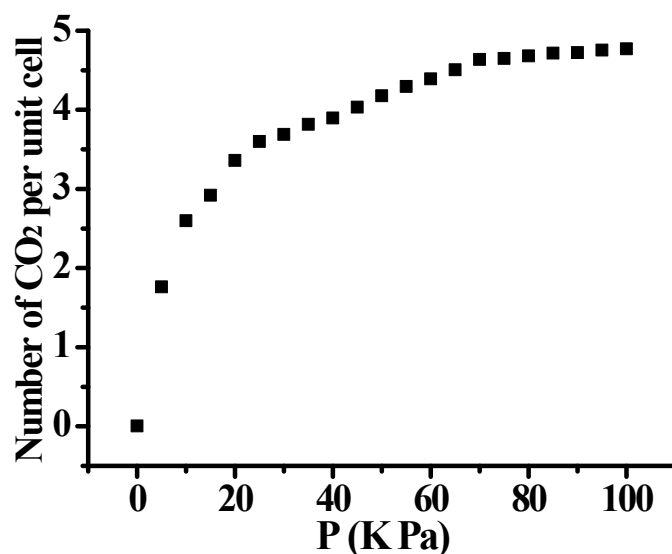


**Figure S8.** Simulated CO<sub>2</sub> adsorption isotherms of **2** at 273K.

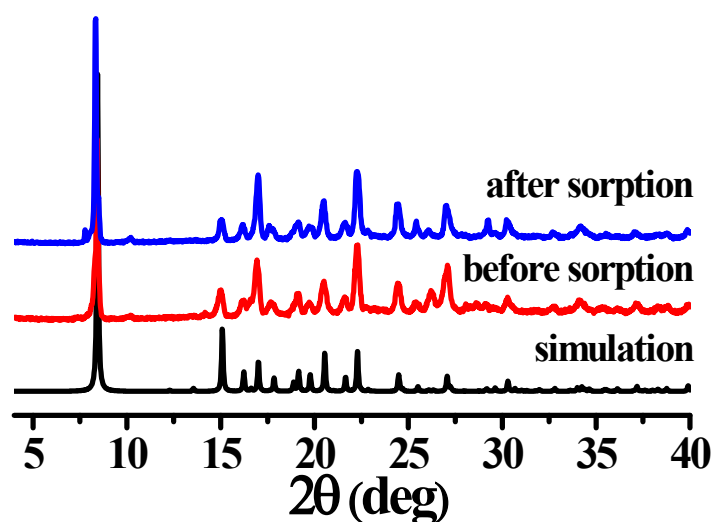


**Figure S9.** The PXRD patterns for **2** before and after CO<sub>2</sub> sorption.

Simulated annealing techniques were used to determine the adsorption sites of CO<sub>2</sub> in the MOF. The framework and the CO<sub>2</sub> molecule were taken as rigid, and the interactions between CO<sub>2</sub> and the framework were evaluated by Lennard-Jones (LJ) and Coulomb potentials. The LJ potentials were taken from the generic universal force field. Partial point charges for framework atoms were calculated using QEq method. To generate proper quadrupole moment of CO<sub>2</sub>, the partial charges on the O and C atoms were set to -0.35e and 0.70e, respectively. A spherical cutoff of 15.5 Å.



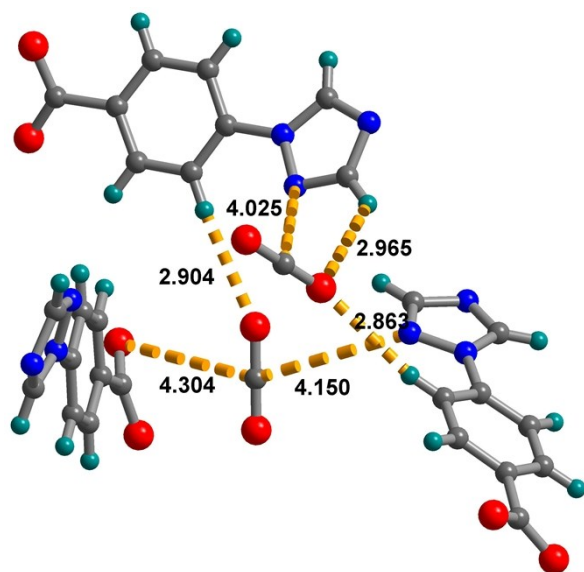


**Figure S10.** Preferred CO<sub>2</sub> adsorption site configurations by annealing simulations. Close contact distances, in Å, are marked.

